



**HAL**  
open science

## Improved histidinylated IPEI polyplexes for skeletal muscle cells transfection

Jean-Pierre Gomez, Guillaume Tresset, Chantal Pichon, Patrick Midoux

### ► To cite this version:

Jean-Pierre Gomez, Guillaume Tresset, Chantal Pichon, Patrick Midoux. Improved histidinylated IPEI polyplexes for skeletal muscle cells transfection. *International Journal of Pharmaceutics*, 2019, 559, pp.58-67. 10.1016/j.ijpharm.2019.01.003 . hal-02067297

**HAL Id: hal-02067297**

**<https://hal.science/hal-02067297>**

Submitted on 21 Oct 2021

**HAL** is a multi-disciplinary open access archive for the deposit and dissemination of scientific research documents, whether they are published or not. The documents may come from teaching and research institutions in France or abroad, or from public or private research centers.

L'archive ouverte pluridisciplinaire **HAL**, est destinée au dépôt et à la diffusion de documents scientifiques de niveau recherche, publiés ou non, émanant des établissements d'enseignement et de recherche français ou étrangers, des laboratoires publics ou privés.



Distributed under a Creative Commons Attribution - NonCommercial 4.0 International License



13 **ABSTRACT**

14 Linear Polyethylenimine (IPEI) is an efficient cationic polymer for transfecting cells, both *in*  
15 *vitro* and *in vivo*, but poses concerns regarding cytotoxicity. Histidinylated IPEI (His-IPEI)  
16 exhibits also high transfection efficiency but lower cytotoxicity than IPEI. For the first time,  
17 we tested polyfection efficiency of polyplexes comprising both IPEI and His-IPEI. A series of  
18 pDNA polyplexes was prepared with mixtures of IPEI and His-IPEI and the amount of each  
19 polymer within His-IPEI/IPEI polyplexes was determined by flow cytometry. We show that  
20 His-IPEI/IPEI polyplexes exhibit properties similar to IPEI polyplexes in terms of size,  
21 morphology, assembly with pDNA, and polyplex stability while His-IPEI/IPEI polyplexes  
22 exhibit properties similar to His-IPEI polyplexes in terms of buffering capacity. Compared to  
23 polyplexes consisting only of IPEI or His-IPEI, the transfection profile reveals that His-  
24 IPEI/IPEI polyplexes containing 30% to 57% IPEI strongly increase polyfection efficiency of  
25 NIH3T3 fibroblasts and murine, as well as human skeletal muscle cell lines without  
26 cytotoxicity. Importantly, improved transfection of human dystrophin deficient skeletal  
27 muscle cell lines was obtained. These results indicate that His-IPEI/IPEI polyplexes are an  
28 improved non-viral vector for efficient transfection of dystrophin deficient skeletal muscle  
29 cell lines that should be tested on animals.

30

31

## 32 **1. Introduction**

33 Gene therapy is an innovative therapeutic approach for treatment of genetic diseases, whether  
34 or not they are inheritable (Thorne et al., 2017). Among the different strategies available for  
35 gene delivery, recombinant viruses are powerful vectors that have significant clinical success  
36 in various pathologies, such as genetic immune severe combined immunodeficiency (X-  
37 SCID), Hemophilia or blinding retinal diseases, such as Leber congenital amaurosis (Dalkara  
38 and Sahel, 2014; Nienhuis et al., 2017). However several obstacles still limit their use,  
39 including immune responses against recombinant viruses, limited length for the transgene  
40 (which is particularly true for AAV, adeno-associated virus), and the expensive cost of their  
41 large-scale industrial production for human application. Chemical vectors, such as cationic  
42 polymers and cationic lipids complexed with plasmid DNA (pDNA) encoding the therapeutic  
43 gene, are a safer approach with higher pDNA loading capacity, lower immunogenicity and  
44 cheaper production, although still less efficient (Donkuru et al., 2010; Jafari et al., 2012;  
45 Junquera and Aicart, 2016; Rezaee et al., 2016; Tros de Ilarduya et al., 2010). Over the last 30  
46 years, cationic polymers have chemically evolved but no molecular structure has emerged as a  
47 new leader (Lachelt and Wagner, 2015). Nowadays, linear polyethylenimine (IPEI) of 22 kDa  
48 is the “gold standard” cationic polymer for transferring pDNA owing to its unique high  
49 property to absorb protons in an acidic medium (Pandey and Sawant, 2016). This buffering  
50 capacity, due to the numerous secondary amino groups present on the polymer backbone,  
51 mediates a proton sponge effect in endosomes allowing escape of pDNA into the cytosol, thus  
52 limiting its lysosomal degradation and enhancing the transfection efficiency (Boussif et al.,  
53 1995; Neuberger and Kichler, 2014). Although IPEI is generally less toxic and exhibits higher  
54 transfection efficiency than its branched (bPEI) counterpart, there is still a certain amount of  
55 cytotoxicity (Castan et al., 2018; Demeneix and Behr, 2005; Gomez et al., 2013; Lungwitz et  
56 al., 2005; Lv et al., 2006). Covalent or non-covalent attachments of various molecules on IPEI

57 enhance its biocompatibility or allow targeting of specific cell populations. In this respect,  
58 poly(ethylene glycol) (PEG), some hydrophobic molecules, pluronic polymers, poly(N-(2-  
59 hydroxypropyl)methacrylamide) derived copolymers, RGD peptides, folic acid, transferrin,  
60 antibodies, saccharides, cyclodextrins, and chitosan/poly(lactic acid) nanoparticles have been  
61 tested (Hobel and Aigner, 2013; Kichler, 2004; Kircheis et al., 2001; Lai et al., 2014; Pandey  
62 and Sawant, 2016). The cytotoxicity was reduced and the transfection efficiency enhanced by  
63 the formation of polyplexes with two polymers, such as  $\gamma$ -polyglutamic acid ( $\gamma$ -PGA) with  
64 bPEI (Kurosaki et al., 2009), bPEI with anionic glycopolymers (Ahmed and Narain, 2013),  
65 polyethylenimine-poly(l-lysine)-poly(l-glutamic acid) (PELG) with hyaluronic acid (He et al.,  
66 2013; Tian et al., 2014; Wang et al., 2011), polyaspartamide with poly(L-lysine) (Sanjoh et  
67 al., 2010), poly (b-amino ester) (PbAE) with carboxymethyl poly (L-histidine) (CM-PLH)  
68 (Gu et al., 2014; Gu et al., 2012), bPEI with poly(methacryloyl sulfadimethoxine) (PSD)-  
69 block-PEG (PSD-b-PEG) (Sethuraman et al., 2006), PEI with chitosan (Jiang et al., 2008;  
70 Zhao et al., 2008), and b-PEI with poly(2-(dimethylamino) ethylmethacrylate (PDMAEMA)  
71 (Lo et al., 2015). Moreover, mixtures of three different polymers, such as poly-l-lysine (PLL)  
72 or Dendrigrift poly-L-lysine (DGL) with poly-l-histidine (PLH) and  $\gamma$ -polyglutamic acid ( $\gamma$ -  
73 PGA) were used to formulate pDNA (Kodama, 2016; Kodama et al., 2015). Multilayered  
74 polyplexes formed by covering (i) DNA/protamine condensate with DNA and finally with  
75 PEI (Qu et al., 2012), (ii) pDNA/PEI or pDNA/poly (N-(8-aminoethyl)-acrylamide) (P8Am)  
76 with poly (acrylic acid) (PAA) and then with bPEI or P8Am (Ke and Young, 2010), enhanced  
77 cell uptake and endosomal escape.

78 In this work, we examined whether the transfection efficiency of histidinylated lPEI (His-  
79 lPEI) polyplexes would increase in the presence of another efficient cationic polymer, such as  
80 lPEI, the closest cationic polymer. His-lPEI exhibits high transfection efficiency, low  
81 cytotoxicity and significant trans-endothelial passage capacity both in normal or inflammatory

82 conditions (Bertrand et al., 2011; Billiet et al., 2012; Gomez et al., 2017; Gomez et al., 2013).  
83 The combination of these powerful cationic polymers has not yet been reported for the  
84 preparation of DNA polyplexes. Remarkably, we found that the combination of His-IPEI and  
85 IPEI gave more efficient polyplexes to transfect fibroblasts and skeletal muscle cells lines  
86 than those consisting only of IPEI or His-IPEI.

## 87 **2. Materials and Methods**

88 All reagents were purchased from Sigma (St. Quentin Fallavier, France) unless otherwise  
89 stated.

### 90 *2.1. Plasmid*

91 p3NFCMVLuc3NF (5556 bp) is a plasmid DNA (pDNA) encoding the firefly luciferase gene  
92 under the control of the human cytomegalovirus (CMV) promoter, with two optimized and  
93 extended NF kappaB DNA binding sequences (3NF) promoting pDNA nuclear import  
94 (Breuzard et al., 2008; Goncalves et al., 2009). Supercoiled plasmid DNA was isolated from  
95 *Escherichia coli* DH5 $\alpha$ <sup>TM</sup> supercompetent bacteria (Invitrogen, Cergy Pontoise, France) by  
96 alkaline lysis and purification was performed by using QIAGEN EndoFree Plasmid Mega Kit  
97 (Qiagen, Courtaboeuf, France).

### 98 *2.2. Cells and cell culture*

99 Cell lines were cultivated at 37°C in a 5% CO<sub>2</sub>-humidified atmosphere. The mouse lung  
100 epithelial cell line (MLE-12 cells; ATCC CRL-2110; Rockville MD, USA) was grown in  
101 HITES medium comprising Dulbecco's Modified Eagle's Medium DMEM/F12 supplemented  
102 with 5  $\mu$ g/ml insulin, 10  $\mu$ g/ml transferrin, 30 nM sodium selenite, 10 nM hydrocortisone, 10  
103 nM  $\beta$ -oestradiol, 10 mM HEPES, 2 mM L-Glutamine, 2 % non-heat inactivated fetal bovine  
104 serum (FBS) and antibiotics (100 units/ml penicillin and 100  $\mu$ g/ml streptomycin). The mouse  
105 embryo fibroblast cell line (NIH3T3 cells, ATCC CRL-1658) was cultured in DMEM 1 g/l  
106 glucose supplemented with 10 % heat-inactivated FBS, 100 units/mL penicillin and 100

107 units/ml streptomycin. The mouse myoblast - C2C12 (CRL1772; ATCC), H2K 2B4 (Muses  
108 et al., 2011) and H2K mdx cell lines (RRID:CVCL\_8120) (Morgan et al., 1994) were cultured  
109 in DMEM 4.5 g/l glucose (PAA) supplemented with 10 % heat-inactivated FBS, 1 % L-  
110 Glutamax, 100 units/mL penicillin and 100 units/ml streptomycin. The normal human  
111 bronchial epithelial cell line (16HBE14o-) (Cozens et al., 1994) (generous gift from Dieter  
112 Gruenert, San Francisco, CA, U.S.A.) was cultured in MEM with Earle's Salts supplemented  
113 with Penicillin (40 Units/ml) and Streptomycin (40 µg/ml), 2mM L-Glutamine and 10% heat-  
114 inactivated FBS. Tissue culture plastic wares were coated for 20-30 min at 37°C with  
115 minimum essential medium (MEM) with Earle's Salts containing fibronectin (0.01 mg/ml),  
116 collagen (0.03 mg/ml) and bovine serum albumin (BSA) (0.1 mg/ml). The culture medium  
117 was changed every 2 days. The human embryo kidney 293T7 cell line (kindly given by Dr L.  
118 Huang) (Brisson et al., 1999) was cultured in DMEM containing 10% FBS, 2 mM L-  
119 glutamine, 1 mM sodium pyruvate, 100 units/mL penicillin, 100 units/ml streptomycin, and  
120 400 µg/ml Geneticin. The human epithelial ovarian carcinoma cell line (HeLa; CCL2, ATCC)  
121 was cultured in MEM supplemented with 10% heat-inactivated FBS, 2mM L-glutamine, 1%  
122 of a 100X non-essential amino acid solution, 100 units/mL penicillin and 100 units/ml  
123 streptomycin. The human normal myoblasts (HSkM) and myoblasts from Duchenne muscular  
124 dystrophic patients (SKM DMD), kindly provided by Dr. V. Mouly (Institut de Myologie,  
125 Paris, France) (Mamchaoui et al., 2011), were cultured in Skeletal muscle cell basal medium  
126 (C-23160, Promocell GmbH, Heidelberg, DE) supplemented with 50 µg/ml bovine fetuin, 10  
127 µg/ml human insulin, 10 ng/ml hEGF (human epidermal growth factor), 1 ng/ml hbFGF  
128 (basic human Fibroblast growth factor), 0.4 µg/ml dexamethasone, 5 % heat-inactivated FBS  
129 (Promocell), 100 units/mL penicillin and 100 units/ml streptomycin. All cell lines were tested  
130 free of mycoplasma by using Mycoalert™ PLUS Mycoplasma Detection kit (Lonza, Basel,  
131 Switzerland).

132 2.3. *Polymers*

133 Linear polyethylenimine (IPEI; Mw of 22 kDa) and His-IPEI (IPEI modified with 16%  
134 histidine residues *per* polymer molecule; Mw of 34.5 kDa) were prepared as described by  
135 (Bertrand et al., 2011). IPEI was labelled with fluorescein. Briefly, 10 mg IPEI dissolved in 1  
136 ml PBS was reacted at room temperature overnight with 1 mg FITC (Invitrogen) dissolved in  
137 0.5 ml DMSO. FITC-IPEI was purified by dialysis (MW 10kDa) against water and then  
138 freeze-dried.

139 2.4. *Polyplexes*

140 Polyplexes made with IPEI, His-IPEI or their mixtures were prepared at DNA/polymer weight  
141 ratio ( $\mu\text{g}/\mu\text{g}$ ) of 1:6. IPEI, His-IPEI or (IPEI + His-IPEI) mixture (30  $\mu\text{g}$  in 30  $\mu\text{l}$  of 10 mM  
142 HEPES buffer, pH 7.4) was added to pDNA (5  $\mu\text{g}$  in 93  $\mu\text{l}$  of 10 mM HEPES buffer, pH 7.4)  
143 and mixed by up-down pipetting. After 4 s vortex mixing, the solution was kept for 30 min at  
144 20°C before use. For transfection, the volume was adjusted to 1 ml with the cell-specific  
145 culture medium.

146 2.5. *Flow cytometry analysis of fluorescent polyplexes*

147 The polymer composition of IPEI/His-IPEI polyplexes was determined by flow cytometry  
148 analysis by using BD LSR FORTRESSA X20 flow cytometer (Becton Dickinson). Polyplexes  
149 made with FITC-PEI/His-IPEI mixtures or FITC-IPEI/IPEI mixture were prepared as  
150 described above and their mean fluorescence intensity (MFI) was measured at  $530 \pm 30$  nm  
151 upon excitation at 488 nm.

152 2.6. *Size and Zeta potential measurements*

153 Polyplexes made with 14  $\mu\text{g}$  DNA were prepared in 1.4 ml of 10 mM HEPES buffer, pH 7.4.  
154 The size was measured at 25°C by quasi-elastic laser light scattering (QELS) with SZ-100  
155 Analyser (Horiba Scientific, les Ulis, France), calibrated with 204 nm latex nanosphere size  
156 standards (Duke Scientific Corps Palo Alto, CA). The  $\zeta$  potential was measured at 25°C by

157 electrophoretic mobility with SZ-100 Analyser, after calibration with DTS 1050 standard  
158 (Malvern).

### 159 2.7. *SYBR Green experiments and Dextran Sulphate competition assays*

160 SYBR Green nucleic acid gel stain (Invitrogen, Thermo Fisher Scientific) was added to  
161 pDNA (2  $\mu$ g) in HEPES buffer (10 mM, pH 7.4) at 1:10000 dilution to obtain a pDNA/SYBR  
162 Green labelled solution. Intercalation-caused fluorescence intensity was quantified using a  
163 Victor I spectrophotometer (PerkinElmer, Courtaboeuf, France) at 520 nm emission and 488  
164 nm excitation and expressed as a percentage of fluorescence in the absence of any polymer. In  
165 Dextran Sulphate (DS) competition assays, pDNA was first labelled with SYBR Green before  
166 polyplex formation, as described above. Dissociation of DNA complexes was then induced by  
167 adding DS (MW of 500 kDa). The fluorescence intensity was measured with a Victor I  
168 spectrophotometer and expressed as the ratio between polyplex fluorescence in the presence  
169 and absence of DS.

### 170 2.8. *CryoTEM*

171 Polyplexes were prepared at a final DNA concentration of 0.15 mg/mL in 10 mM HEPES, pH  
172 7.4. A Quantifoil R2/2 carbon grid (Jena, Germany) was ionized by glow discharge and 3  $\mu$ L  
173 of polyplexes was deposited onto it. The grid was then abruptly immersed in liquid ethane *via*  
174 a FEI Vitrobot cryoplunger and stored in liquid nitrogen until use. The frozen samples were  
175 introduced into a high resolution JEOL-2010 transmission electron microscope equipped with  
176 a 200-kV field emission gun via a Gatan 626 cryoholder. They were imaged at a  
177 magnification of 50,000x using a minimal dose system enabling film exposure while  
178 preserving the samples from beam damage. The images were collected with a Gatan Ultrascan  
179 4K CCD camera with a defocus of 1  $\mu$ m.

180

181

## 182 2.9. *Transfection*

183 Two days before transfection, cells were seeded in 24 well culture plates at a density of  $1 \times 10^5$   
184 to  $1.5 \times 10^5$  cells/cm<sup>2</sup> depending on the cell lines used. At the time of transfection, the culture  
185 medium was discarded and the cells were incubated with 1 ml of polyplexes (5 µg/ml pDNA).  
186 After 4 h, the medium was removed and cells were cultured in their standard culture medium.  
187 The transfection efficiency was quantified after 48 h post-transfection by measuring the  
188 luciferase activity in cell lysates as follows. The culture medium was removed and cells were  
189 lysed at room temperature during 10 min in lysis buffer (1 % Triton X-100, 25 mM Tris-  
190 phosphate, 1 mM DTT, 1 mM EDTA, 15 % glycerol, 1 mM MgCl<sub>2</sub>, pH 7.8). Luciferase  
191 substrate (Beetle luciferin, Promega, Madison, USA) was added to the lysate supernatant in  
192 the presence of 1 mM ATP. The luciferase activity was measured using a luminometer  
193 (Lumat LB 9507, Berthold, Thoiry, France) and expressed as RLU *per* mg of protein after  
194 protein normalization using the BCA colorimetric assay and bovine serum albumin.

## 195 2.10. *Cytotoxicity*

196 The cytotoxicity of polyplexes was measured after 48 h post-transfection by using the MTT  
197 assay (Mosmann, 1983). 3-(4,5-dimethylthiazol-2-yl)-2,5-diphenyltetrazolium bromide  
198 (MTT; 100 µl of 5 mg/mL solution in PBS) was added *per* culture well. After 4 h incubation  
199 at 37°C, MTT converted in formazan was solubilized with acidic isopropanol. The absorbance  
200 at 570 nm was measured with Victor I spectrophotometer and cytotoxicity expressed as a  
201 percentage of absorbance relative to control cells (cells without any treatments).

## 202 2.11. *Statistics*

203 The results were expressed as the mean ± standard deviation. The mean of each group was  
204 compared by the non-parametric Mann-Whitney statistical test.  $p < 0.05$  was considered as  
205 statistically significant.

206

### 207 3. Results

#### 208 3.1. Physicochemical characterization of IPEI / His-IPEI polyplexes

209 A series of polyplexes was prepared with pDNA and mixtures of IPEI and His-IPEI. The  
210 pDNA/polymer weight ratio was kept constant and equal to 1/6 (N/P of 4.88), a value which  
211 had demonstrated strong DNA condensation and high transfection efficiency in several cell  
212 lines (Bertrand et al., 2011; Goncalves et al., 2016). His-IPEI/IPEI polyplexes were prepared  
213 by varying the percentage of His-IPEI and IPEI from 0% IPEI (100% His-IPEI) to 100% IPEI  
214 (0% His-IPEI) at N/P ratios ranged from 4.88 to 9.18. First, polyplex formation was  
215 characterized by agarose gel electrophoresis shift assay. Independent of the nature of the  
216 polymer mixtures, no pDNA migrated, indicating its total complexation with the polymers  
217 and polymer mixtures (Fig. 1). The electrophoresis band in the well was more fluorescent  
218 with His-IPEI than with IPEI, revealing better pDNA condensation with the latter polymer  
219 than the former. The fluorescence intensity of wells corresponding to His-IPEI polyplexes  
220 containing IPEI was weak in line with an enhanced pDNA condensation (Fig. 1). To further  
221 characterize the polyplexes, their size was measured by DLS (Fig. 2). His-IPEI formed  
222 polyplexes of  $90 \pm 10$  nm. The size of polyplexes with IPEI/His-IPEI mixture decreased as  
223 IPEI quantity increased in the mixture, from  $83 \pm 2.3$  nm at N/P of 5.31 to  $65.8 \pm 2$  nm at N/P  
224 of 8.75, a size value close to that of IPEI polyplexes ( $65 \pm 1.4$  nm). The  $\xi$  potential did not  
225 differ significantly between the various polymer mixtures and was in the range of 25 mV to  
226 38 mV, similar to the polyplexes consisting only of IPEI ( $34.2 \pm 8$  mV) or His-IPEI ( $33.2 \pm$   
227  $0.6$  mV) (Fig. 3).

#### 228 3.2. Interaction strength between pDNA and His-IPEI, IPEI or His-IPEI/IPEI

229 As observed in agarose gel electrophoresis, pDNA condensation varied with the polymer  
230 mixture composition. Dye exclusion assay was performed to obtain more information. pDNA  
231 was stained with SYBR Green and then the fluorescence intensity was measured after

232 addition of IPEI or His-IPEI or their mixtures. The fluorescence intensity of IPEI/His-IPEI  
233 polyplexes decreased as the IPEI quantity increased, from 87 % at N/P of 5.31 to 95 % at N/P  
234 of 8.75, confirming an increased in pDNA condensation (Fig. 4). In contrast, fluorescence  
235 decrease in the presence of IPEI reached 98 % whereas it was only of 76 % in the presence of  
236 His-IPEI in line with agarose gel electrophoresis. These values corresponded to maximal and  
237 minimal pDNA condensation.

### 238 3.3. *Polymer composition within polyplexes*

239 At pH 7.4, IPEI and His-IPEI exhibit 102 and 85 cationic charges *per* polymer molecule,  
240 respectively (Bertrand et al., 2011). Therefore, IPEI interacts more strongly with pDNA than  
241 His-IPEI at the same concentration. Consequently, the percentages of IPEI and His-IPEI  
242 complexed with pDNA within the same polyplex cannot be the same as in the original  
243 polymer mixture. In order to determine the amount of IPEI and His-IPEI that are effectively  
244 associated with pDNA within polyplexes, the composition in polyplexes was assessed by flow  
245 cytometry analysis of polyplexes using FITC-IPEI (Fig. 5). First, the mean fluorescence  
246 intensity (MFI) of polyplexes made with FITC-IPEI/IPEI was measured as a function of the  
247 amount of FITC-IPEI and non-fluorescent IPEI. Figure 5A & 5B showed that MFI decreased  
248 linearly when the amount of non-fluorescent IPEI increased in the polymer mixture  
249 corresponding to a FITC-IPEI dilution effect by IPEI. This meant that interaction with pDNA  
250 of FITC-IPEI and non-fluorescent IPEI was identical. In contrast, the MFI of FITC-IPEI/His-  
251 IPEI polyplexes did not decrease linearly when the amount of non-fluorescent His-IPEI  
252 increased (Fig. 5B). This indicated that the interaction with pDNA of FITC-IPEI and non-  
253 fluorescent His-IPEI was different. As expected, IPEI interacts stronger than His-IPEI in line  
254 with its higher amount of cationic charges. The real amount of IPEI and His-IPEI within  
255 IPEI/His-IPEI polyplexes was determined from the FITC-IPEI/IPEI polyplex curve (Table 1).  
256 The results indicated that polyplexes contained 30% and 73% IPEI when the mixture

257 comprised 15% and 51% IPEI, respectively. Above 70% IPEI in the mixture, the polyplexes  
258 contained only IPEI.

### 259 3.4. *Buffering capacity*

260 Endosome destabilization by IPEI and His-IPEI is a common property of these two polymers.  
261 Thus, the buffering capacities of the HisIPEI/IPEI mixture (molar ratio of 72/28; %/%)  
262 estimated by measuring the change in pH of the polymer solution upon titration with 0.1N  
263 HCl solution was compared to that of IPEI and His-IPEI and (Fig. 6). The buffering capacity  
264 is proportional to the reciprocal slope of the titration plot over a pH range. The titration curve  
265 of IPEI over the pH range of 4 to 8 presents one phase with a reciprocal slope of 47.6 ml. In  
266 contrast, there are two phases in the titration curve of His-IPEI and the mixture. The buffering  
267 capacity of His-IPEI was 36.7 ml in the pH range of 4 to 6.3, which was slightly lower than  
268 that of IPEI. In contrast, it was higher (135 ml) than that of IPEI in the pH range of 6 to 7.4  
269 related to the pH range of endosomes. The buffering capacity of the mixture in the pH range  
270 of 4 to 6.5 (29.5 ml) was slightly lower than that of His-IPEI in the same pH range whereas it  
271 was closer to that of His-IPEI in the pH range of endosomes (109 ml). Compared to His-IPEI,  
272 the reduced buffering capacity of the mixture in the two pH ranges was due to the presence of  
273 IPEI.

### 274 3.5. *Polyplex stability*

275 The stability of the polyplexes was tested by measuring their fluorescence intensity in the  
276 presence of DS, a polyanion of high molecular weight (500 kDa) (Fig. 7). The addition of 2  
277  $\mu\text{M}$  DS drastically increased the intensity of SYBR Green fluorescence from a ratio of 1 to 4  
278 for IPEI polyplexes and His-IPEI/IPEI polyplexes containing 30% and 57% IPEI, indicating  
279 that decondensation and/or release of pDNA occurred. In contrast, the fluorescence intensity  
280 of His-IPEI polyplexes did not change whatever the DS concentration, indicating a greater  
281 stability of these polyplexes compared to those consisting only of IPEI.

### 282 3.6. *Polyplex morphology*

283 The supramolecular structures of His-IPEI/IPEI polyplexes made with 72% of His-IPEI and  
284 28% IPEI were investigated by cryo-transmission electron microscopy (cryo-TEM). His-  
285 IPEI/IPEI polyplexes micrographs showed the characteristic toroidal wrapping of DNA with a  
286 clear short-range organization (Fig. 8a & 8b). This organization was similar to that of  
287 polyplexes consisting only of IPEI (Fig. 8c) but contrast with that of polyplexes consisting of  
288 only His-IPEI that did not show any DNA organization, as previously reported (Fig. 8d)  
289 (Maury et al., 2014).

### 290 3.7. *Transfection efficiency of IPEI / His-IPEI polyplexes*

291 The transfection efficiency of IPEI/His-IPEI polyplexes was assessed in various cell lines with  
292 pDNA encoding the luciferase reporter gene. In NIH 3T3 cells, the luciferase expression upon  
293 transfection with His-IPEI polyplexes was  $3.9 \times 10^5$  RLU per mg of protein (Fig. 9). The  
294 luciferase activity increased progressively upon transfection with IPEI/His-IPEI polyplexes  
295 containing an increasing amount of IPEI and reached a value 200-fold higher than that  
296 obtained with His-IPEI polyplexes. When polyplexes contained 27% His-IPEI and 73% IPEI,  
297 the luciferase activity reached a maximum of  $8.5 \times 10^7$  RLU/mg of protein, a value close to  
298 that obtained with IPEI polyplexes ( $4.5 \times 10^7$  RLU/mg of protein).

299 The transfection efficiency profile of H2K mdx cells was different (Fig. 10). In the first place,  
300 His-IPEI polyplexes were more efficient than IPEI polyplexes ( $3.7 \times 10^6$  versus  $1.1 \times 10^5$   
301 RLU/mg protein). On the other hand, the efficiency of His-IPEI/IPEI polyplexes containing  
302 30% IPEI and 70% His-IPEI was ~12-fold higher compared to His-IPEI polyplexes. The  
303 addition of a higher proportion of IPEI did not offer any additional benefit, since the  
304 transfection efficiency gradually decreased to reach a value ( $3.5 \times 10^5$  RLU/mg protein) close  
305 to that of IPEI polyplexes, in line with the fact that above 70% IPEI, polyplexes contained  
306 only IPEI. When assessed by MTT assay, IPEI polyplexes displayed high cytotoxicity ( $77.5 \pm$

307 1 %) on H2K mdx cells in contrast to His-IPEI polyplexes ( $20 \pm 2$  %) (Fig. 11). The  
308 cytotoxicity of His-IPEI/IPEI polyplexes appeared when His-IPEI/IPEI polyplexes contained  
309 73% IPEI and increased progressively to reach a cytotoxicity close to that of polyplexes  
310 consisting of only IPEI. The IC<sub>50</sub>% of cytotoxicity of IPEI was 30, 6.5, 20 and 6.5  $\mu\text{g/ml}$  on  
311 HeLa, HEK293T7, C2C12 and  $\Sigma\text{CFTE}$  cells, respectively whereas it was  $\gg 100$   $\mu\text{g/ml}$  for  
312 His-IPEI (Bertrand et al., 2011). Accordingly, in His-IPEI/IPEI polyplexes made with polymer  
313 mixtures containing less than 70% IPEI, a large amount of IPEI was associated with pDNA,  
314 thus contributing to a reduction in cytotoxicity. Above 70% IPEI, however, the polyplex  
315 solution contained mostly free IPEI, which was responsible for the cytotoxicity. In summary,  
316 His-IPEI/IPEI polyplexes containing less than 70% IPEI presented a benefit in terms of  
317 transfection efficiency and viability of H2K mdx cells.

318 Next, the transfection efficiency of His-IPEI/IPEI polyplexes was evaluated on various murine  
319 and human cell lines (Tables 2 and 3). There was no beneficial effect in the mouse lung  
320 epithelial MLE-12 cells (Table 2). Conversely, His-IPEI/IPEI polyplexes were more effective  
321 than His-IPEI and IPEI polyplexes in mouse muscular cells. Transfection increased 6.5- to  
322 6.7-fold in normal myoblasts (C2C12 cells) and immortal satellite cell-derived from  
323 myofibres (H2K 2B4 cells) with His-IPEI/IPEI polyplexes containing 30 to 57 % IPEI and  
324 11.6-fold in dystrophic cells (H2K mdx cells). A similar transfection profile was observed in  
325 human cell lines (Table 3). There was no benefit for transfection from His-IPEI/IPEI  
326 polyplexes in non-muscular cells, such as the epithelial ovarian carcinoma cells (HeLa cells)  
327 and the human embryo kidney cells (293T7 cells). A weak benefit (1.24-fold) was observed in  
328 human bronchial epithelial cells (16HBE14o- cells) in the presence of 30% IPEI. However,  
329 His-IPEI/IPEI polyplexes containing 30 % IPEI enhanced  $\sim 3$ -fold the transfection of normal  
330 (SKMH cells) and dystrophic (SKM DMD cells) myoblasts.

331

#### 332 4. Discussion

333 In the present study, the transfection efficiency of polyplexes consisting of both His-IPEI and  
334 IPEI demonstrated superiority in NIH3T3 cells and skeletal muscle cells in comparison to  
335 polyplexes consisting only of IPEI or His-IPEI. The presence of IPEI within His-IPEI  
336 polyplexes increased pDNA condensation in line with its higher amount of cationic charges  
337 providing stronger interaction with pDNA rather than His-IPEI. This higher condensation was  
338 observed by agarose gel electrophoresis showing lower dye inclusion in pDNA and by  
339 dynamic light scattering showing hydrodynamic size reduction of His-IPEI polyplexes in the  
340 presence of IPEI. The  $\zeta$  potential of His-IPEI/IPEI polyplexes was not modified and was in  
341 the range of 24.8 mV to 38.4 mV, close to that of polyplexes consisting only of His-IPEI or  
342 IPEI. The presence of IPEI within His-IPEI polyplexes decreased polyplex stability suggesting  
343 that the supramolecular assembly was different from that of His-IPEI polyplexes. DNA  
344 compaction varies with the type of cationic polymers, the number of cationic charges *per*  
345 polymer molecule, and the nature of the chemical group bearing the cationic charges, leading  
346 to structurally different supramolecular assemblies with pDNA. High-resolution cryo-TEM  
347 images previously showed that histidinylation of IPEI had a crucial influence on polyplex  
348 morphology. His-IPEI polyplexes exhibited a spherical shape and amorphous character  
349 indicating that the binding energy of partners was weaker than in the ordered globular  
350 structures of IPEI polyplexes (Maury et al., 2014). The same results were obtained by Cryo-  
351 TEM analyses in the present study. Here, Cryo-TEM of polyplexes consisting of 72% His-  
352 IPEI and 28% IPEI showed that their well-ordered structure was similar to that of IPEI  
353 polyplexes. DNA condensation by cationic polymers is reversible in the presence of high  
354 molecular weight polyanions (Sun et al., 2011a; Sun et al., 2011b). When tested, DS of high  
355 molecular weight allowed dissociation of IPEI polyplexes and His-IPEI/IPEI polyplexes but  
356 not His-IPEI polyplexes. While DNA compaction or packaging is a relatively slow process,

357 DNA decondensation is a rapid process occurring in a few seconds upon its initialization  
358 (Widom and Baldwin, 1980). Therefore, decondensation of the well-ordered structure  
359 required lower amounts of polyanion than in unordered structures. Compared to polyplexes  
360 consisting only of His-IPEI, the presence of IPEI within His-IPEI polyplexes decreased their  
361 stability in the presence of DS, suggesting that IPEI could control the assembly of polyplexes  
362 containing both polymers. This confirms the Cryo-TEM images, which show organizational  
363 similarity between His-IPEI/IPEI/DNA complexes and IPEI/DNA complexes. Here, the  
364 polyplexes were formed by mixing pDNA with the mixture of two polymers at different  
365 percentages. Interaction of pDNA with IPEI is greater compared to His-IPEI due to its higher  
366 number of cationic charges. Flow cytometry allowed the determination of the amount of each  
367 polymer really associated with the polyplexes. This determination was essential and  
368 confirmed that competition occurred between the two polymers. The preparation of His-  
369 IPEI/IPEI polyplexes was different to that of multi-layered polyplexes, where the polyplexes  
370 were formed with a first polymer before addition of the second polymer interacting with the  
371 polyplex surface. Here, the interactions of His-IPEI and IPEI with the nucleic acid occur at the  
372 same time and form an ordered assembly probably without polymer multilayers.

373 The impact of His-IPEI/IPEI polyplexes on transfection was assessed in various murine and  
374 human cell lines. Transfection was performed in NIH3T3 mouse fibroblasts because a  
375 superior transgene expression (~10-fold) was reported in this cell line transfected with  
376 polyplexes made with a PDMAEMA/PEI mixture at a ratio 1:9 compared to polyplexes  
377 containing PDMAEMA or PEI (Lo et al., 2015). IPEI/His-IPEI polyplexes revealed also better  
378 transfection efficiency (up to 200-fold) than polyplexes consisting only of IPEI or His-IPEI in  
379 NIH3T3 mouse fibroblasts. The transfection was one order of magnitude higher than with  
380 PDMAEMA/PEI polyplexes. Transfections of bronchial epithelial cells and skeletal muscle  
381 cells were evaluated because these cell lines are relevant in the Cystic Fibrosis and Duchenne

382 Muscular Dystrophy gene therapy field. His-IPEI/IPEI polyplexes improved the transfection  
383 of murine or human skeletal muscle cell lines by 4.3- to 11.5- fold in C2C12 and H2K mdx  
384 cell lines and by 3-fold in SKM and SKM DMD cell lines. These results are interesting since  
385 proliferating myoblasts are usually difficult to transfect with non-viral systems, such as  
386 calcium phosphate precipitation, cationic lipid reagents and many cationic polymers.  
387 Transfection efficiency typically varies between 10 and 30% (Jackson et al., 2013).  
388 Improvements of the transgene expression in C2C12 cells have been reported with polyplexes  
389 made with hyperbranched poly(ester amine)s (PEAs) (Wang et al., 2012) and with PEI and  
390 the amphipathic peptide KALA (Min et al., 2006). We did not observe significant  
391 improvement in the other cell lines including bronchial epithelial cells. At this stage, it is  
392 unclear why His-IPEI/IPEI polyplexes transfected fibroblasts and skeletal muscle cells more  
393 efficiently than the other cell lines. The fact that fibroblasts are convertible into cells of the  
394 skeletal muscle lineage (Bar-Nur et al., 2018) and C2C12 or NIH/3T3 cells can differentiate  
395 into chondrogenic and osteogenic lineages in vitro (Li et al., 2005) could suggest common  
396 cell behavior.

397

## 398 **5. Conclusion**

399 The combination of the His-IPEI and l-PEI polymers for DNA polyplexes preparation has not  
400 previously been reported. Remarkably, we found that some IPEI/His-IPEI combinations lead  
401 to performant and non-cytotoxic polyplexes for fibroblast and skeletal muscle cell  
402 transfection. His-IPEI/IPEI polyplexes exhibited properties similar to IPEI polyplexes in terms  
403 of size, morphology, assembly with pDNA and stability, while His-IPEI/IPEI polyplexes  
404 exhibited properties similar to His-IPEI polyplexes in terms of buffering capacity. At this  
405 stage, it is unclear why His-IPEI/IPEI polyplexes transfected fibroblasts and skeletal muscle  
406 cells more efficiently than the other cell lines. Deeper investigations are required to determine

407 which specific properties of His-IPEI/IPEI polyplexes contribute to the improved effect  
408 observed with these cells. The evaluation of other cationic polymers could determine whether  
409 this effect is restricted to the His-IPEI/PEI couple. IPEI/His-IPEI polyplexes that showed  
410 particular efficacy in dystrophic skeletal muscle cells should be tested to transfer the  
411 dystrophin gene in mdx animals.

412

### 413 **Conflict of interest statement**

414 The authors declare that they have no conflict of interest.

### 415 **Acknowledgements**

416 We thank Virginie Malard for buffering capacity measurements, David Gosset and the  
417 “Cytometry and Cell Imaging” P@CYFIC platform” at CBM. We thank Jénil Degrouard for  
418 his technical assistance with the electron microscope. The electron microscopy imaging was  
419 supported by “Investissements d’Avenir” LabEx PALM (ANR-10-LABX-0039-PALM). We  
420 are grateful to Frances Westall (CBM) for editing the manuscript. This work was supported  
421 by grants from ‘Association Française contre les Myopathies’ (Strategic project 2009,  
422 #15628AFM (AFM, Evry, France).

423

424

425

426

427

428

429

430

431

432           **References**

- 433           • Ahmed, M., Narain, R., 2013. Cell line dependent uptake and transfection efficiencies  
434           of PEI-anionic glycopolymer systems. *Biomaterials* 34, 4368-4376.
- 435           • Bar-Nur, O., Gerli, M.F.M., Di Stefano, B., Almada, A.E., Galvin, A., Coffey, A.,  
436           Huebner, A.J., Feige, P., Verheul, C., Cheung, P., Payzin-Dogru, D., Paisant, S.,  
437           Anselmo, A., Sadreyev, R.I., Ott, H.C., Tajbakhsh, S., Rudnicki, M.A., Wagers, A.J.,  
438           Hochedlinger, K., 2018. Direct Reprogramming of Mouse Fibroblasts into Functional  
439           Skeletal Muscle Progenitors. *Stem Cell Reports* 10, 1505-1521.
- 440           • Bertrand, E., Goncalves, C., Billiet, L., Gomez, J.P., Pichon, C., Cheradame, H.,  
441           Midoux, P., Guegan, P., 2011. Histidinylated linear PEI: a new efficient non-toxic  
442           polymer for gene transfer. *Chem Commun (Camb)* 47, 12547-12549.
- 443           • Billiet, L., Gomez, J.P., Berchel, M., Jaffres, P.A., Le Gall, T., Montier, T., Bertrand,  
444           E., Cheradame, H., Guegan, P., Mevel, M., Pitard, B., Benvegny, T., Lehn, P., Pichon,  
445           C., Midoux, P., 2012. Gene transfer by chemical vectors, and endocytosis routes of  
446           polyplexes, lipoplexes and lipopolyplexes in a myoblast cell line. *Biomaterials* 33,  
447           2980-2990.
- 448           • Boussif, O., Lezoualc'h, F., Zanta, M.A., Mergny, M.D., Scherman, D., Demeneix, B.,  
449           Behr, J.P., 1995. A versatile vector for gene and oligonucleotide transfer into cells in  
450           culture and in vivo: polyethylenimine. *Proc Natl Acad Sci U S A* 92, 7297-7301.
- 451           • Breuzard, G., Tertilt, M., Goncalves, C., Cheradame, H., Guegan, P., Pichon, C.,  
452           Midoux, P., 2008. Nuclear delivery of NFkappaB-assisted DNA/polymer complexes:  
453           plasmid DNA quantitation by confocal laser scanning microscopy and evidence of  
454           nuclear polyplexes by FRET imaging. *Nucleic Acids Res* 36, e71.
- 455           • Brisson, M., He, Y., Li, S., Yang, J.P., Huang, L., 1999. A novel T7 RNA polymerase  
456           autogene for efficient cytoplasmic expression of target genes. *Gene Ther* 6, 263-270.

- 457 • Castan, L., Jose da Silva, C., Ferreira Molina, E., Alves Dos Santos, R., 2018.  
458 Comparative study of cytotoxicity and genotoxicity of commercial Jeffamines(R) and  
459 polyethylenimine in CHO-K1 cells. *J Biomed Mater Res B Appl Biomater* 106, 742-  
460 750.
- 461 • Cozens, A.L., Yezzi, M.J., Kunzelmann, K., Ohrui, T., Chin, L., Eng, K., Finkbeiner,  
462 W.E., Widdicombe, J.H., Gruenert, D.C., 1994. CFTR expression and chloride  
463 secretion in polarized immortal human bronchial epithelial cells. *Am J Respir Cell*  
464 *Mol Biol* 10, 38-47.
- 465 • Dalkara, D., Sahel, J.A., 2014. Gene therapy for inherited retinal degenerations. *C R*  
466 *Biol* 337, 185-192.
- 467 • Demeneix, B., Behr, J.P., 2005. Polyethylenimine (PEI). *Adv Genet* 53, 217-230.
- 468 • Donkuru, M., Badea, I., Wettig, S., Verrall, R., Elsbahy, M., Foldvari, M., 2010.  
469 Advancing nonviral gene delivery: lipid- and surfactant-based nanoparticle design  
470 strategies. *Nanomedicine (Lond)* 5, 1103-1127.
- 471 • Gomez, J.P., Goncalves, C., Pichon, C., Midoux, P., 2017. Effect of IL-1beta, TNF-  
472 alpha and IGF-1 on trans-endothelial passage of synthetic vectors through an in vitro  
473 vascular endothelial barrier of striated muscle. *Gene Ther* 24, 416-424.
- 474 • Gomez, J.P., Pichon, C., Midoux, P., 2013. Ability of plasmid DNA complexed with  
475 histidinylated IPEI and IPEI to cross in vitro lung and muscle vascular endothelial  
476 barriers. *Gene* 525, 182-190.
- 477 • Goncalves, C., Akhter, S., Pichon, C., Midoux, P., 2016. Intracellular Availability of  
478 pDNA and mRNA after Transfection: A Comparative Study among Polyplexes,  
479 Lipoplexes, and Lipopolyplexes. *Mol Pharm* 13, 3153-3163.

- 480 • Goncalves, C., Ardourel, M.Y., Decoville, M., Breuzard, G., Midoux, P., Hartmann,  
481 B., Pichon, C., 2009. An optimized extended DNA kappa B site that enhances plasmid  
482 DNA nuclear import and gene expression. *J Gene Med* 11, 401-411.
- 483 • Gu, J., Chen, X., Xin, H., Fang, X., Sha, X., 2014. Serum-resistant complex  
484 nanoparticles functionalized with imidazole-rich polypeptide for gene delivery to  
485 pulmonary metastatic melanoma. *Int J Pharm* 461, 559-569.
- 486 • Gu, J., Wang, X., Jiang, X., Chen, Y., Chen, L., Fang, X., Sha, X., 2012. Self-  
487 assembled carboxymethyl poly (L-histidine) coated poly (beta-amino ester)/DNA  
488 complexes for gene transfection. *Biomaterials* 33, 644-658.
- 489 • He, Y., Cheng, G., Xie, L., Nie, Y., He, B., Gu, Z., 2013. Polyethyleneimine/DNA  
490 polyplexes with reduction-sensitive hyaluronic acid derivatives shielding for targeted  
491 gene delivery. *Biomaterials* 34, 1235-1245.
- 492 • Hobel, S., Aigner, A., 2013. Polyethylenimines for siRNA and miRNA delivery in  
493 vivo. *Wiley Interdiscip Rev Nanomed Nanobiotechnol* 5, 484-501.
- 494 • Jackson, M.F., Hoversten, K.E., Powers, J.M., Trobridge, G.D., Rodgers, B.D., 2013.  
495 Genetic manipulation of myoblasts and a novel primary myosatellite cell culture  
496 system: comparing and optimizing approaches. *FEBS J* 280, 827-839.
- 497 • Jafari, M., Soltani, M., Naahidi, S., Karunaratne, D.N., Chen, P., 2012. Nonviral  
498 approach for targeted nucleic acid delivery. *Curr Med Chem* 19, 197-208.
- 499 • Jiang, H.L., Kim, T.H., Kim, Y.K., Park, I.Y., Cho, M.H., Cho, C.S., 2008. Efficient  
500 gene delivery using chitosan-polyethylenimine hybrid systems. *Biomed Mater* 3,  
501 025013.
- 502 • Junquera, E., Aicart, E., 2016. Recent progress in gene therapy to deliver nucleic acids  
503 with multivalent cationic vectors. *Adv Colloid Interface Sci* 233, 161-175.

- 504 • Ke, J.H., Young, T.H., 2010. Multilayered polyplexes with the endosomal buffering  
505 polycation in the core and the cell uptake-favorable polycation in the outer layer for  
506 enhanced gene delivery. *Biomaterials* 31, 9366-9372.
- 507 • Kichler, A., 2004. Gene transfer with modified polyethylenimines. *J Gene Med* 6  
508 Suppl 1, S3-10.
- 509 • Kircheis, R., Wightman, L., Wagner, E., 2001. Design and gene delivery activity of  
510 modified polyethylenimines. *Adv Drug Deliv Rev* 53, 341-358.
- 511 • Kodama, Y., 2016. Development of a Multi-functional Nano-device for Safe and  
512 Effective Gene Delivery to Target Organs. *Yakugaku Zasshi* 136, 1533-1539.
- 513 • Kodama, Y., Yatsugi, Y., Kitahara, T., Kurosaki, T., Egashira, K., Nakashima, M.,  
514 Muro, T., Nakagawa, H., Higuchi, N., Nakamura, T., Sasaki, H., 2015. Quaternary  
515 complexes modified from pDNA and poly-l-lysine complexes to enhance pH-  
516 buffering effect and suppress cytotoxicity. *J Pharm Sci* 104, 1470-1477.
- 517 • Kurosaki, T., Kitahara, T., Fumoto, S., Nishida, K., Nakamura, J., Niidome, T.,  
518 Kodama, Y., Nakagawa, H., To, H., Sasaki, H., 2009. Ternary complexes of pDNA,  
519 polyethylenimine, and gamma-polyglutamic acid for gene delivery systems.  
520 *Biomaterials* 30, 2846-2853.
- 521 • Lachelt, U., Wagner, E., 2015. Nucleic Acid Therapeutics Using Polyplexes: A  
522 Journey of 50 Years (and Beyond). *Chem Rev* 115, 11043-11078.
- 523 • Lai, W.F., Green, D.W., Jung, H.S., 2014. Linear poly(ethylenimine) cross-linked by  
524 methyl-beta-cyclodextrin for gene delivery. *Curr Gene Ther* 14, 258-268.
- 525 • Li, G., Peng, H., Corsi, K., Usas, A., Olshanski, A., Huard, J., 2005. Differential effect  
526 of BMP4 on NIH/3T3 and C2C12 cells: implications for endochondral bone  
527 formation. *J Bone Miner Res* 20, 1611-1623.

- 528 • Lo, C.W., Liao, W.H., Wu, C.H., Lee, J.L., Sun, M.K., Yang, H.S., Tsai, W.B.,  
529 Chang, Y., Chen, W.S., 2015. Synergistic Effect of PEI and PDMAEMA on  
530 Transgene Expression in Vitro. *Langmuir* 31, 6130-6136.
- 531 • Lungwitz, U., Breunig, M., Blunk, T., Gopferich, A., 2005. Polyethylenimine-based  
532 non-viral gene delivery systems. *Eur J Pharm Biopharm* 60, 247-266.
- 533 • Lv, H., Zhang, S., Wang, B., Cui, S., Yan, J., 2006. Toxicity of cationic lipids and  
534 cationic polymers in gene delivery. *J Control Release* 114, 100-109.
- 535 • Mamchaoui, K., Trollet, C., Bigot, A., Negroni, E., Chaouch, S., Wolff, A., Kandalla,  
536 P.K., Marie, S., Di Santo, J., St Guily, J.L., Muntoni, F., Kim, J., Philippi, S., Spuler,  
537 S., Levy, N., Blumen, S.C., Voit, T., Wright, W.E., Aamiri, A., Butler-Browne, G.,  
538 Mouly, V., 2011. Immortalized pathological human myoblasts: towards a universal  
539 tool for the study of neuromuscular disorders. *Skelet Muscle* 1, 34.
- 540 • Maury, B., Goncalves, C., Tresset, G., Zeghal, M., Cheradame, H., Guegan, P.,  
541 Pichon, C., Midoux, P., 2014. Influence of pDNA availability on transfection  
542 efficiency of polyplexes in non-proliferative cells. *Biomaterials* 35, 5977-5985.
- 543 • Min, S.H., Lee, D.C., Lim, M.J., Park, H.S., Kim, D.M., Cho, C.W., Yoon, D.Y.,  
544 Yeom, Y.I., 2006. A composite gene delivery system consisting of polyethylenimine  
545 and an amphipathic peptide KALA. *J Gene Med* 8, 1425-1434.
- 546 • Morgan, J.E., Beauchamp, J.R., Pagel, C.N., Peckham, M., Ataliotis, P., Jat, P.S.,  
547 Noble, M.D., Farmer, K., Partridge, T.A., 1994. Myogenic cell lines derived from  
548 transgenic mice carrying a thermolabile T antigen: a model system for the derivation  
549 of tissue-specific and mutation-specific cell lines. *Dev Biol* 162, 486-498.
- 550 • Mosmann, T., 1983. Rapid colorimetric assay for cellular growth and survival:  
551 application to proliferation and cytotoxicity assays. *J Immunol Methods* 65, 55-63.

- 552 • Muses, S., Morgan, J.E., Wells, D.J., 2011. A new extensively characterised  
553 conditionally immortal muscle cell-line for investigating therapeutic strategies in  
554 muscular dystrophies. PLoS One 6, e24826.
- 555 • Neuberg, P., Kichler, A., 2014. Recent developments in nucleic acid delivery with  
556 polyethylenimines. Adv Genet 88, 263-288.
- 557 • Nienhuis, A.W., Nathwani, A.C., Davidoff, A.M., 2017. Gene Therapy for  
558 Hemophilia. Mol Ther 25, 1163-1167.
- 559 • Pandey, A.P., Sawant, K.K., 2016. Polyethylenimine: A versatile, multifunctional non-  
560 viral vector for nucleic acid delivery. Mater Sci Eng C Mater Biol Appl 68, 904-918.
- 561 • Qu, X., Li, P., Liu, D., Liu, C., Zhang, N., 2012. Enhanced gene transfer with  
562 multilayered polyplexes assembled with layer-by-layer technique. IET  
563 Nanobiotechnol 6, 122-128.
- 564 • Rezaee, M., Oskuee, R.K., Nassirli, H., Malaekheh-Nikouei, B., 2016. Progress in the  
565 development of lipopolyplexes as efficient non-viral gene delivery systems. J Control  
566 Release 236, 1-14.
- 567 • Sanjoh, M., Hiki, S., Lee, Y., Oba, M., Miyata, K., Ishii, T., Kataoka, K., 2010.  
568 pDNA/poly(L-lysine) Polyplexes Functionalized with a pH-Sensitive Charge-  
569 Conversional Poly(aspartamide) Derivative for Controlled Gene Delivery to Human  
570 Umbilical Vein Endothelial Cells. Macromol Rapid Commun 31, 1181-1186.
- 571 • Sethuraman, V.A., Na, K., Bae, Y.H., 2006. pH-responsive sulfonamide/PEI system  
572 for tumor specific gene delivery: an in vitro study. Biomacromolecules 7, 64-70.
- 573 • Sun, C., Tang, T., Uludag, H., 2011a. Molecular dynamics simulations of PEI  
574 mediated DNA aggregation. Biomacromolecules 12, 3698-3707.

- 575 • Sun, C., Tang, T., Uludag, H., Cuervo, J.E., 2011b. Molecular dynamics simulations  
576 of DNA/PEI complexes: effect of PEI branching and protonation state. *Biophys J* 100,  
577 2754-2763.
- 578 • Thorne, B., Takeya, R., Vitelli, F., Swanson, X., 2017. Gene Therapy. *Adv Biochem*  
579 *Eng Biotechnol*, 1-49.
- 580 • Tian, H., Guo, Z., Lin, L., Jiao, Z., Chen, J., Gao, S., Zhu, X., Chen, X., 2014. pH-  
581 responsive zwitterionic copolypeptides as charge conversional shielding system for  
582 gene carriers. *J Control Release* 174, 117-125.
- 583 • Tros de Ilarduya, C., Sun, Y., Duzgunes, N., 2010. Gene delivery by lipoplexes and  
584 polyplexes. *Eur J Pharm Sci* 40, 159-170.
- 585 • Wang, M., Tucker, J.D., Lu, P., Wu, B., Cloer, C., Lu, Q., 2012. Tris[2-  
586 (acryloyloxy)ethyl]isocyanurate cross-linked low-molecular-weight polyethylenimine  
587 as gene delivery carriers in cell culture and dystrophic mdx mice. *Bioconjug Chem* 23,  
588 837-845.
- 589 • Wang, Y., Xu, Z., Zhang, R., Li, W., Yang, L., Hu, Q., 2011. A facile approach to  
590 construct hyaluronic acid shielding polyplexes with improved stability and reduced  
591 cytotoxicity. *Colloids Surf B Biointerfaces* 84, 259-266.
- 592 • Widom, J., Baldwin, R.L., 1980. Cation-induced toroidal condensation of DNA  
593 studies with  $\text{Co}^{3+}(\text{NH}_3)_6$ . *J Mol Biol* 144, 431-453.
- 594 • Zhao, Q.Q., Chen, J.L., Han, M., Liang, W.Q., Tabata, Y., Gao, J.Q., 2008.  
595 Combination of poly(ethylenimine) and chitosan induces high gene transfection  
596 efficiency and low cytotoxicity. *J Biosci Bioeng* 105, 65-68.

597

598

599 **LEGENDS OF FIGURES**

600 **Figure 1: Agarose gel electrophoresis shift assay of pDNA complexed with His-IPEI,**  
601 **IPEI alone or IPEI/HisIPEI at different molar ratios.** N/P stands for the pDNA/polymer  
602 charge (negative to positive) ratios assuming that at pH 7.4, IPEI and His-IPEI exhibited 102  
603 and 85 cationic charges per polymer molecule, respectively (Bertrand et al., 2011). pDNA  
604 free or complexed with the polymers was analyzed on a 0.6% agarose gel. Gel running buffer  
605 was TAE (40 mM Tris-acetate, 1 mM EDTA) and pDNA gel was stained with ethidium  
606 bromide (EtBr) at a concentration of 0.5 µg/ml.

607  
608 **Figure 2: Size of pDNA complexed with His-IPEI, IPEI or IPEI/HisIPEI at different**  
609 **molar ratios.** Dashed line is the fit curve between size measurements values and IPEI/His-  
610 IPEI molar ratio. (▲) is N/P values as a function of IPEI/HisIPEI molar ratio. Values are  
611 means ± SD.

612  
613 **Figure 3: ζ potential of pDNA complexed with His-IPEI, IPEI or IPEI/HisIPEI at**  
614 **different molar ratios.** (▲) is N/P values as a function of IPEI/HisIPEI molar ratio. Values  
615 are means ± SD.

616  
617 **Figure 4: Dye exclusion assay.** The fluorescence of 2 µg pDNA in the presence of SYBR  
618 Green in HEPES buffer was measured in the presence of various quantities of His-IPEI, IPEI  
619 or IPEI/HisIPEI. Fluorescence intensity is expressed as the percent of fluorescence in the  
620 absence of any polymer. (▲) is N/P values as a function of IPEI/HisIPEI molar ratio. Values  
621 are means ± SD.

622

623 **Figure 5: Polymers composition of polyplexes.** A series of FITC-IPEI/IPEI polyplexes and  
624 FITC-IPEI/His-IPEI polyplexes was prepared as a function of the polymers molar ratio in the  
625 mixture. The mean fluorescence intensity (MFI) of polyplexes was measured by flow  
626 cytometry (488 nm excitation; 520 nm emission). (A) Fluorescence histograms of FITC-  
627 IPEI/IPEI polyplexes containing (red) 70%, (yellow) 50%, (blue) 30% and (green) 0% non-  
628 fluorescent IPEI. (B) Variation of the MFI of (●) FITC-IPEI/IPEI and (▲) FITC-IPEI/His-  
629 IPEI polyplexes expressed as  $MFI/MFI_{100}$  where  $MFI_{100}$  corresponds to polyplexes containing  
630 100% of FITC-IPEI. Dashed line corresponds to the linear regression fit of MFI of FITC-  
631 IPEI/IPEI polyplexes.

632

633 **Figure 6: Titration of polymer solutions with 0.1 N HCl.** Solutions of 3 mg/ml (□) IPEI,  
634 (●) His-IPEI or (▲) the HisIPEI/IPEI mixture (molar ratio of 72/28; %/%) were adjusted to  
635 pH = 12 with 0.1 N NaOH, then 20 ml aliquots of 0.1 N HCl were progressively added and  
636 the pH measured.

637

638 **Figure 7: Polyplexes stability.** pDNA in the presence of SYBR Green (1 : 10000) in 10 mM  
639 HEPES buffer, pH 7.4 was complexed at DNA/polymer molar ratio of 1/6 either with (□)  
640 IPEI, (●) His-IPEI or IPEI/His-IPEI mixture containing (Δ) 30% or (▲) 57% IPEI. Then, the  
641 fluorescence intensity was measured in the absence and in the presence of various amounts of  
642 Dextran Sulphate (DS) of 500 kDa molecular weight. The fluorescence intensity was  
643 expressed as the ratio between fluorescence of polyplexes in the presence to that in the  
644 absence of DS. Values are means  $\pm$  SD.

645

646 **Figure 8: Cryo-TEM micrographs** of (a and b) His-IPEI/IPEI, (c) IPEI and (d) His-IPEI  
647 polyplexes. Scale bar is 50 nm.

648

649 **Figure 9: Transfection efficiency of NIH3T3 cells.** The cells were transfected with IPEI-,  
650 HisIPEI- or IPEI/HisIPEI polyplexes containing pDNA encoding the luciferase gene (5  
651  $\mu\text{g/ml}$ ). The luciferase activity in cell lysates was measured 48 h post-transfection and  
652 expressed as relative light units (RLU) *per* mg of protein. ( $\blacktriangle$ ) is N/P values as a function of  
653 IPEI/His-IPEI molar ratio. Values are means  $\pm$  SD. (\*:  $p < 0.05$  *versus* IPEI;  $\diamond$  :  $p < 0.05$  *versus*  
654 His-IPEI).

655

656 **Figure 10: Transfection efficiency of H2K mdx cells.** The cells were transfected with IPEI-  
657 , His-IPEI- or IPEI/HisIPEI polyplexes containing pDNA encoding the luciferase gene (5  
658  $\mu\text{g/ml}$ ). The luciferase activity in cell lysates was measured 48 h post-transfection and  
659 expressed as relative light units (RLU) *per* mg of protein. ( $\blacktriangle$ ) is N/P values as a function of  
660 IPEI/His-IPEI molar ratio. Values are means  $\pm$  SD. (\*:  $p < 0.05$  *versus* IPEI).

661

662 **Figure 11: Cytotoxicity in H2K mdx cells.** The cells were transfected with IPEI-, HisIPEI-  
663 or IPEI/His-IPEI polyplexes as in Fig. 10. The cytotoxicity was measured 48 h post-  
664 transfection using MTT assay and the percentage of cytotoxicity is expressed relatively to  
665 non-transfected cells. ( $\blacktriangle$ ) is N/P values as a function of IPEI/His-IPEI molar ratio. Values are  
666 means  $\pm$  SD. (\*\*:  $p < 0.01$  *versus* IPEI;  $\diamond\diamond$  :  $p < 0.01$  *versus* His-IPEI).

667

668

669

670

671

672

673

674

675

**Table 1: Molar quantity of His-IPEI and IPEI associated to polyplexes (%)**

in the mixture		within polyplexes	
His-IPEI	IPEI	His-IPEI	IPEI
100	0	100	0
85	15	70 ± 4	30 ± 2
72	28	43 ± 2	57 ± 3
59	41	33 ± 2	67 ± 4
49	51	27 ± 2	73 ± 3
39	61	15 ± 1	85 ± 5
30	70	3 ± 0.5	97 ± 3
22	78	0	100
14	86	0	100
7	93	0	100
0	100	0	100

676

677

678

679

680

681

682

683

684

685

**Table 2 : His-IPEI/PEI polyplexes improvement on transfection of mouse cell lines**

Polyplexes		Cell lines					
His-IPEI	IPEI	RLU His-IPEI/PEI polyplexes /RLU His-IPEI polyplexes					
(%)	(%)	N/P	MLE-12	NiH3T3	C2C12	H2K 2B4	H2K mdx
100	0	4.88	1	1	1	1	1
70	30	5.31	0.6	5.5	6.5	6.7	11.5
43	57	5.74	0.1	51	7.0	6.8	7.6
33	67	6.32	0.4	130	4.3	6.4	4.2
27	73	6.6	0.2	212	3.1	8.5	1.9
15	85	7.08	0.15	208	3.2	5.1	0.8
3	97	7.45	0.1	249	4	4.4	0.5
0	100	9.18	0.01	114	3.1	1.0	0.03

686 Data shown corresponds to representative experiment performed in triplicate and reproduced  
687 at least three times. RLU is the relative light unit per mg of protein  
688

689

690

691

692

693

694

695

696

697

698

699

**Table 3 : His-IPEI/PEI polyplexes improvement on transfection of human cell lines**

Polyplexes		Cell lines					
His-IPEI	IPEI	RLU His-IPEI/PEI polyplexes /RLU His-IPEI polyplexes					
(%)	(%)	N/P	16HBE14o-	293T7	HeLa	SKMH	SKM DMD
100	0	4.88	1	1	1	1	1
70	30	5.31	1.2	0.9	0.6	3.2	2.9
43	57	5.74	0.70	0.6	0.15	0.7	0.1
33	67	6.32	0.5	0.8	0.25	0.15	0.02
27	73	6.6	0.5	0.5	0.40	0.1	0.1
15	85	7.08	0.6	0.3	0.46	0.2	0.04
3	97	7.45	0.5	0.2	0.71	0.1	0.01
0	100	9.18	0.2	0.1	0.42	0.001	-

700 Data shown corresponds to representative experiment performed in triplicate and reproduced  
701 at least three times. . RLU is the relative light unit per mg of protein  
702

703

704

705

0	0	1107	996	885	775	664	553	443	350	221	111	His-IPEI/DNA (mol)
0	1735	0	174	347	549	694	868	1041	1215	1388	1562	IPEI/DNA (mol)
0/100	100/0	85/15	72/28	59/41	49/51	39/61	30/70	22/78	14/86	7/93		His-IPEI/IPEI molar ratio (%)
	9.18	4.88	5.31	5.74	6.32	6.6	7.08	7.45	8.00	8.31	8.75	N/P

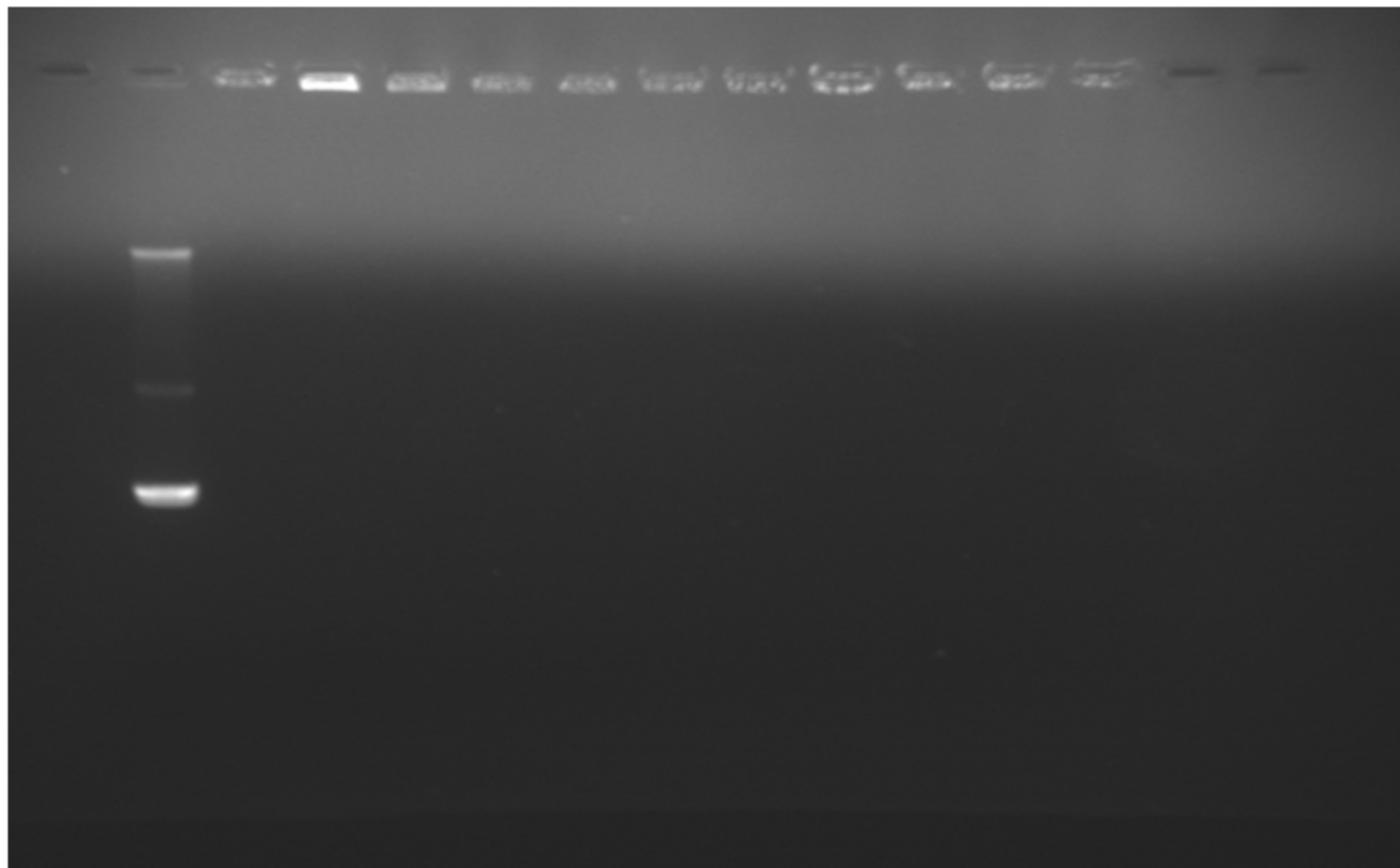


Fig 1

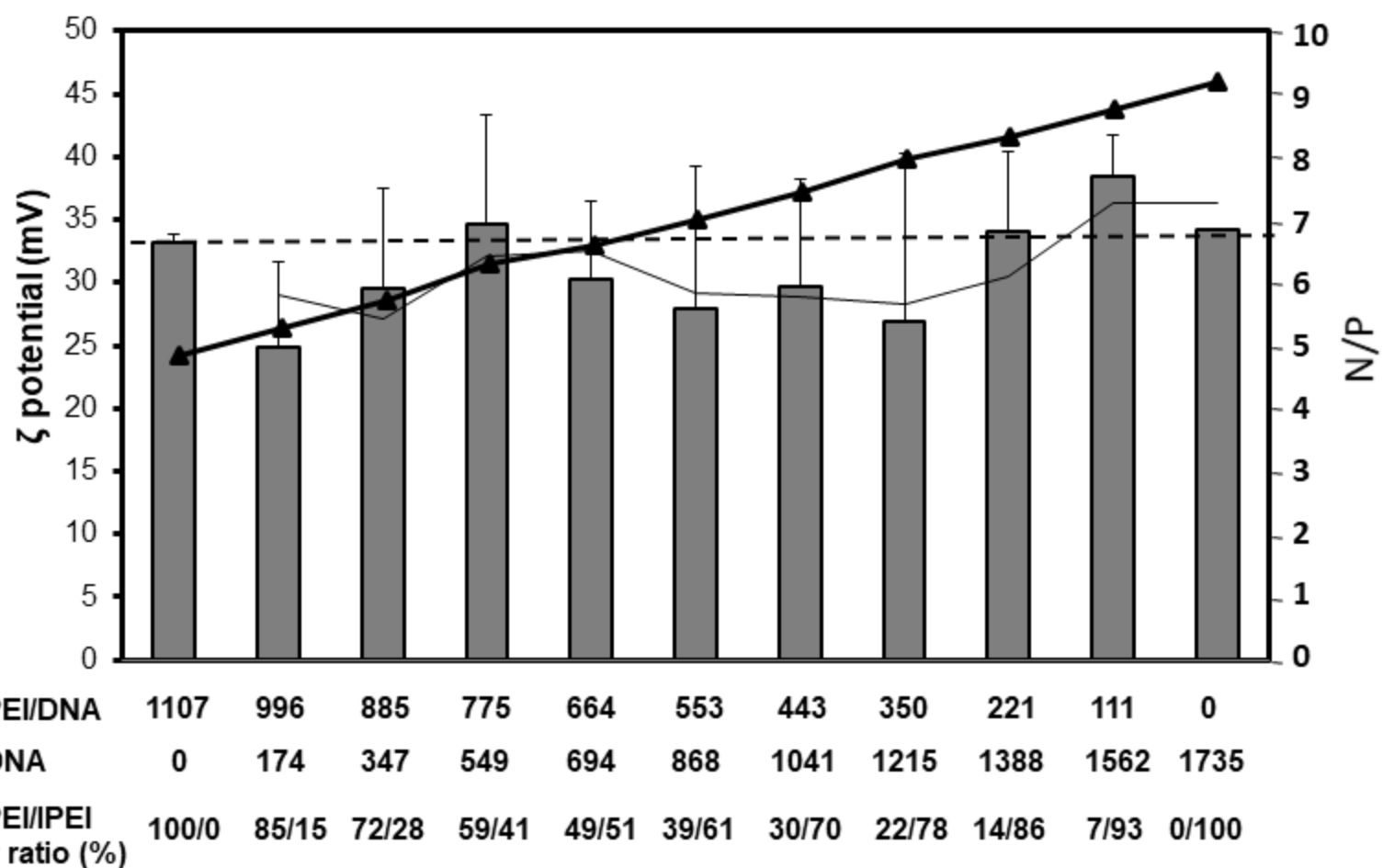


Fig 3

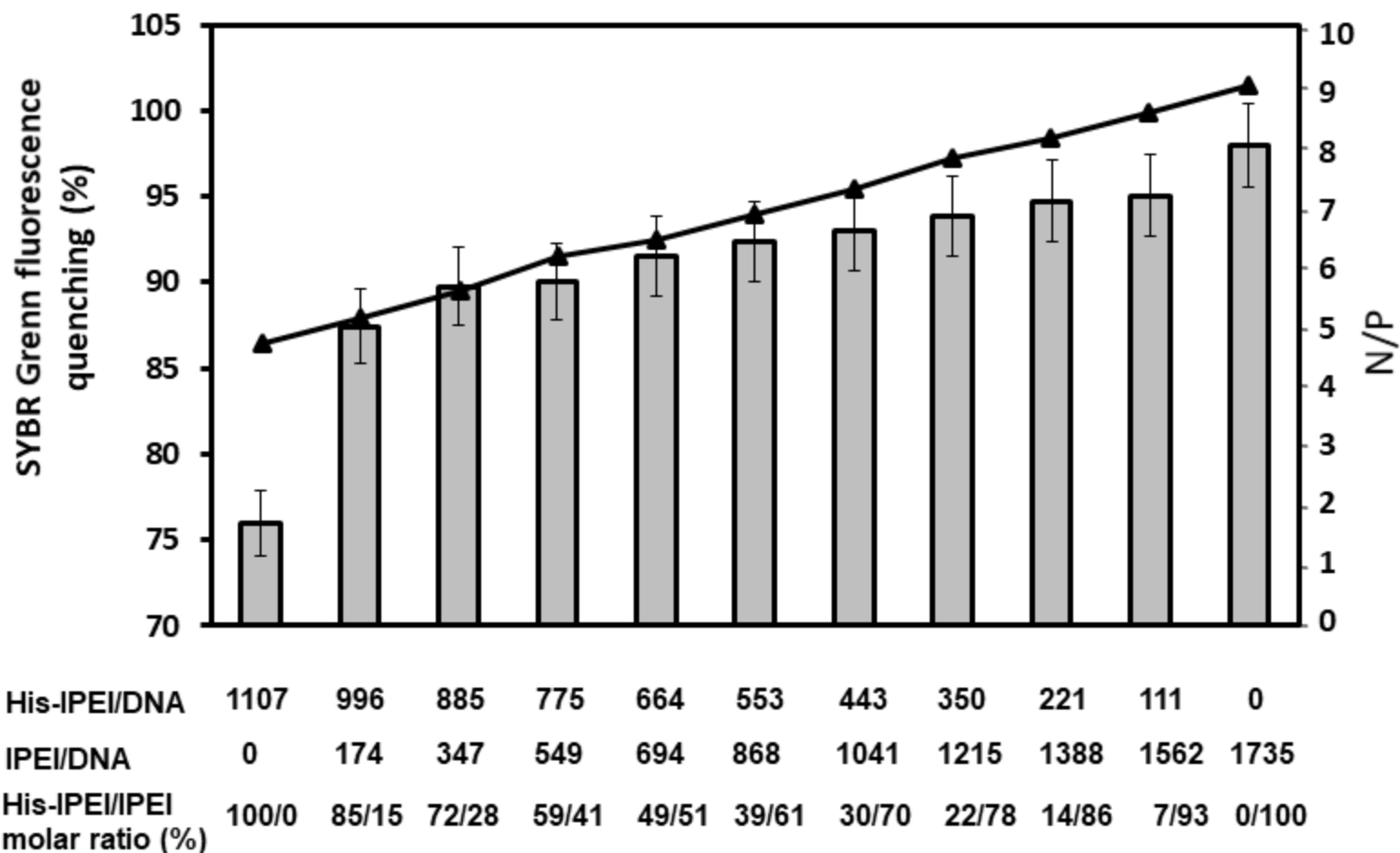


Fig 4

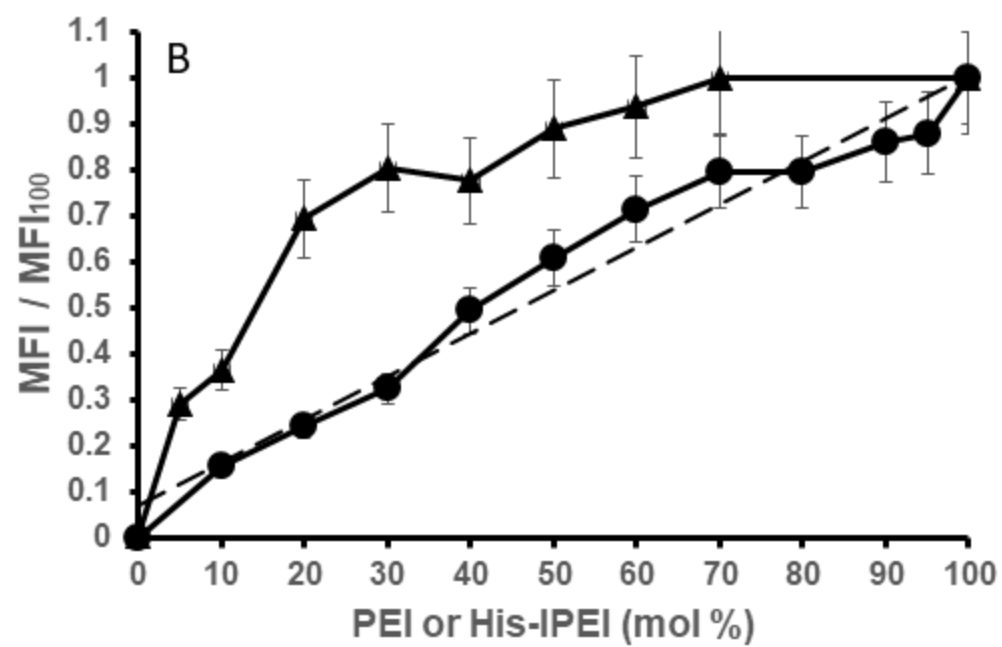
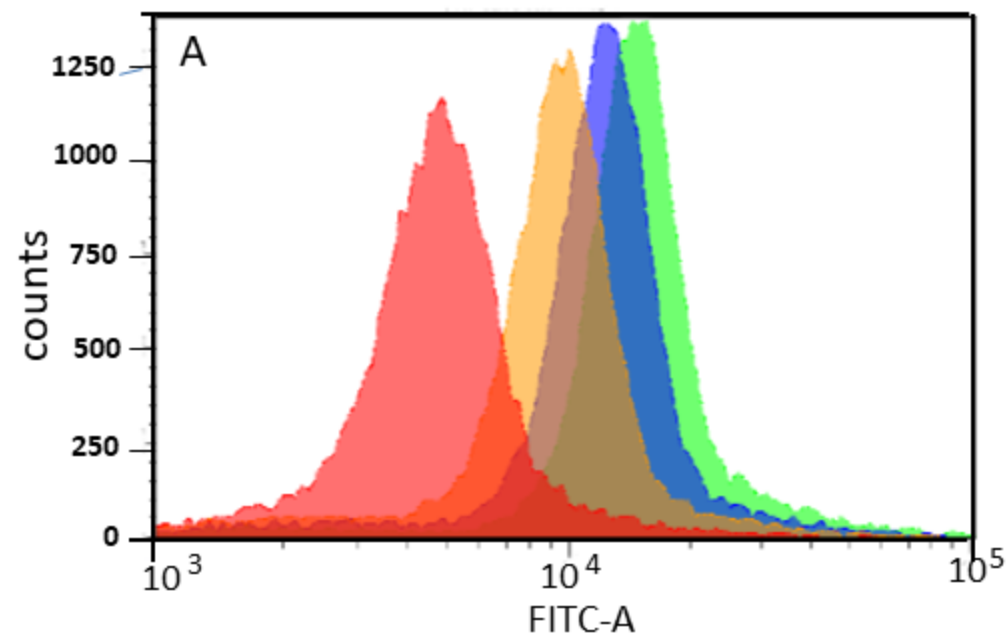


Fig 5

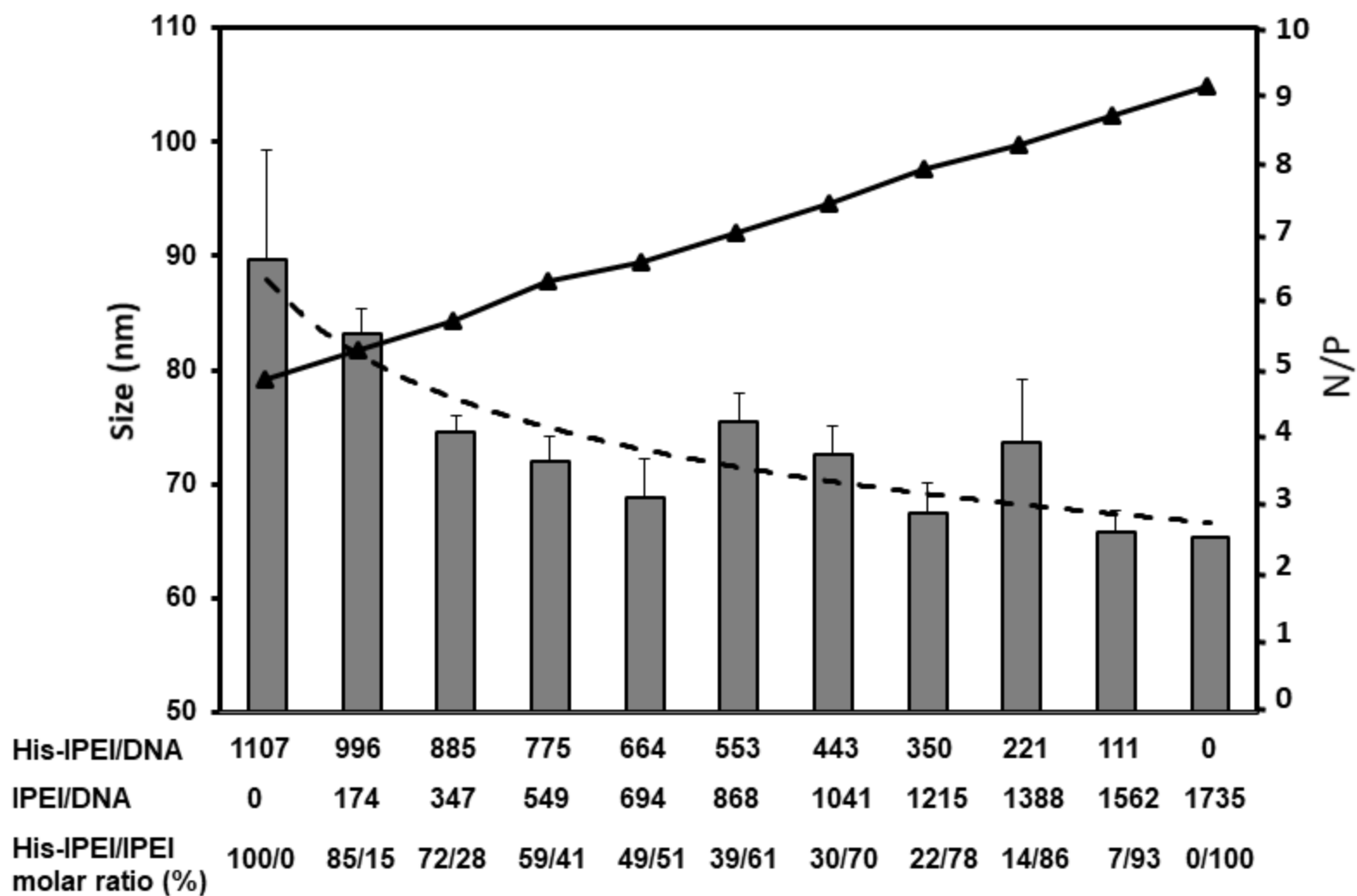


Fig 2

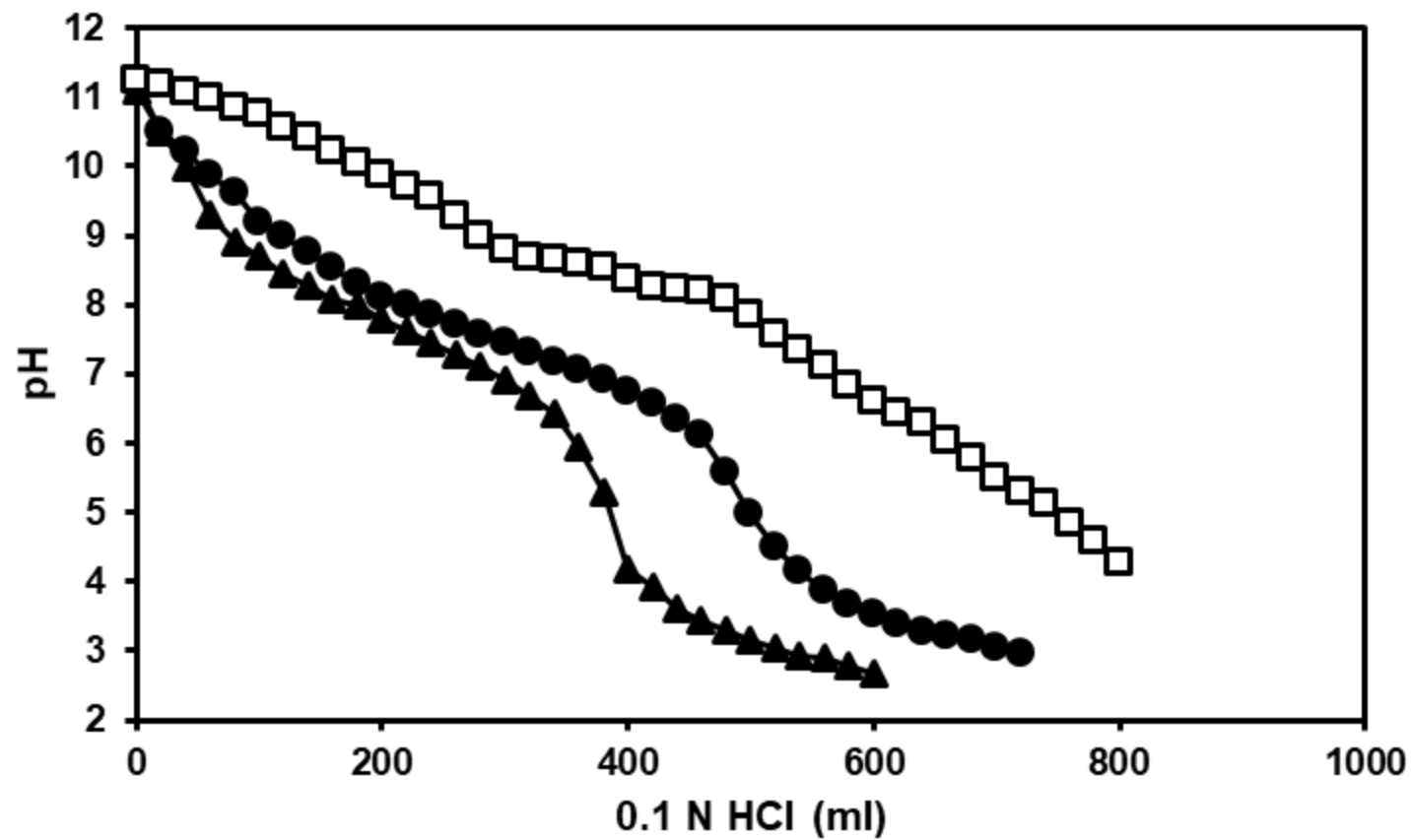


Fig 6

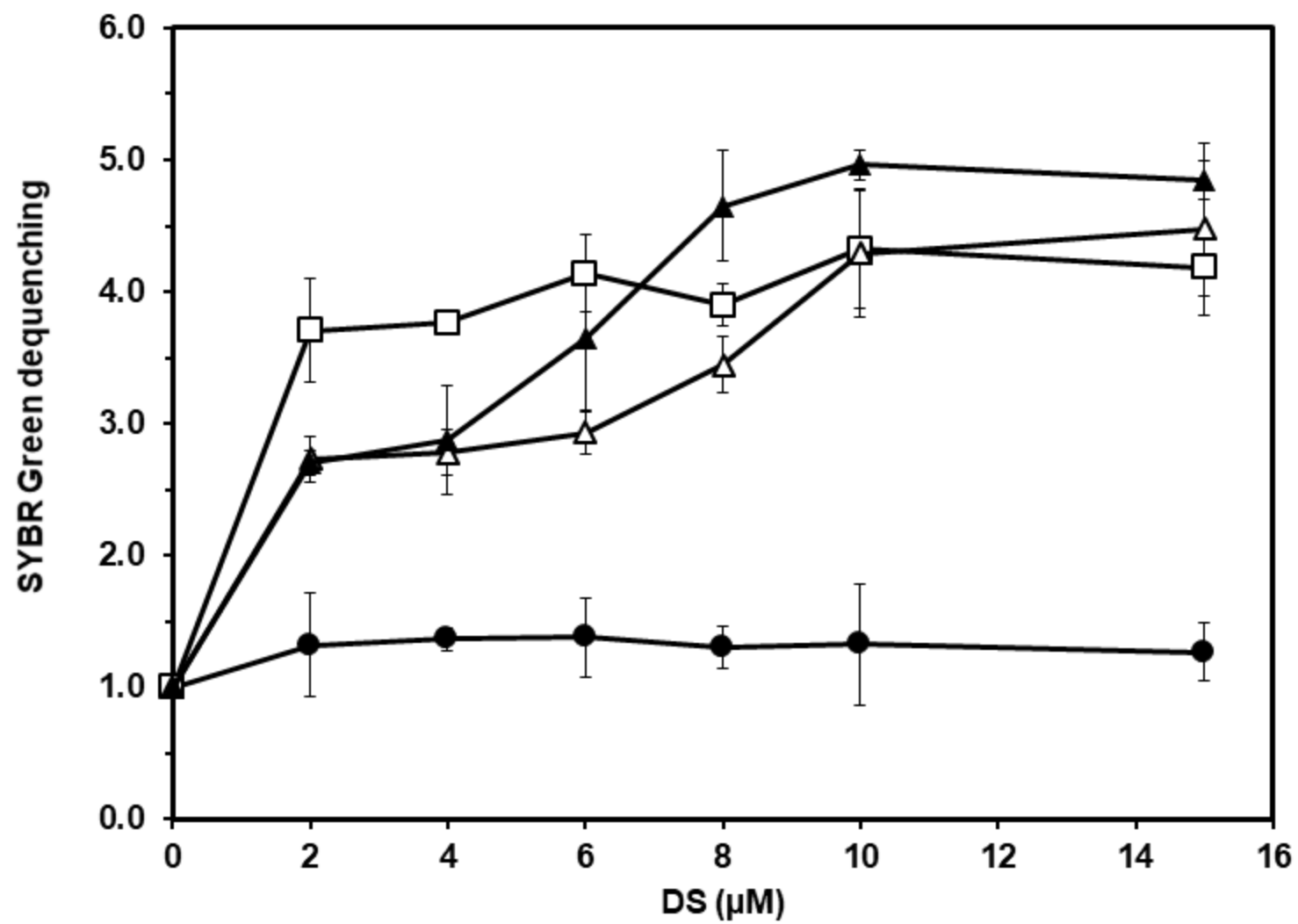
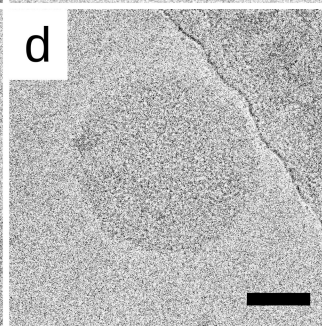
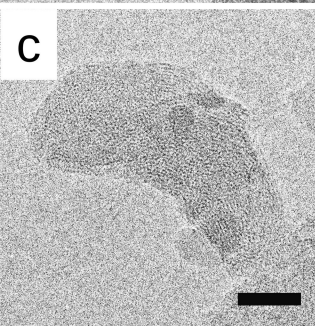
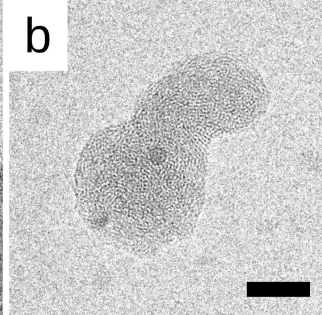
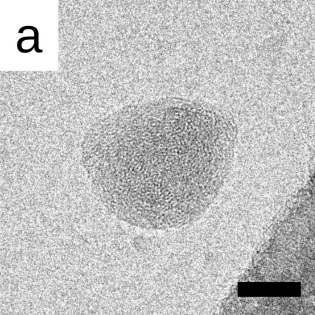


Fig 7



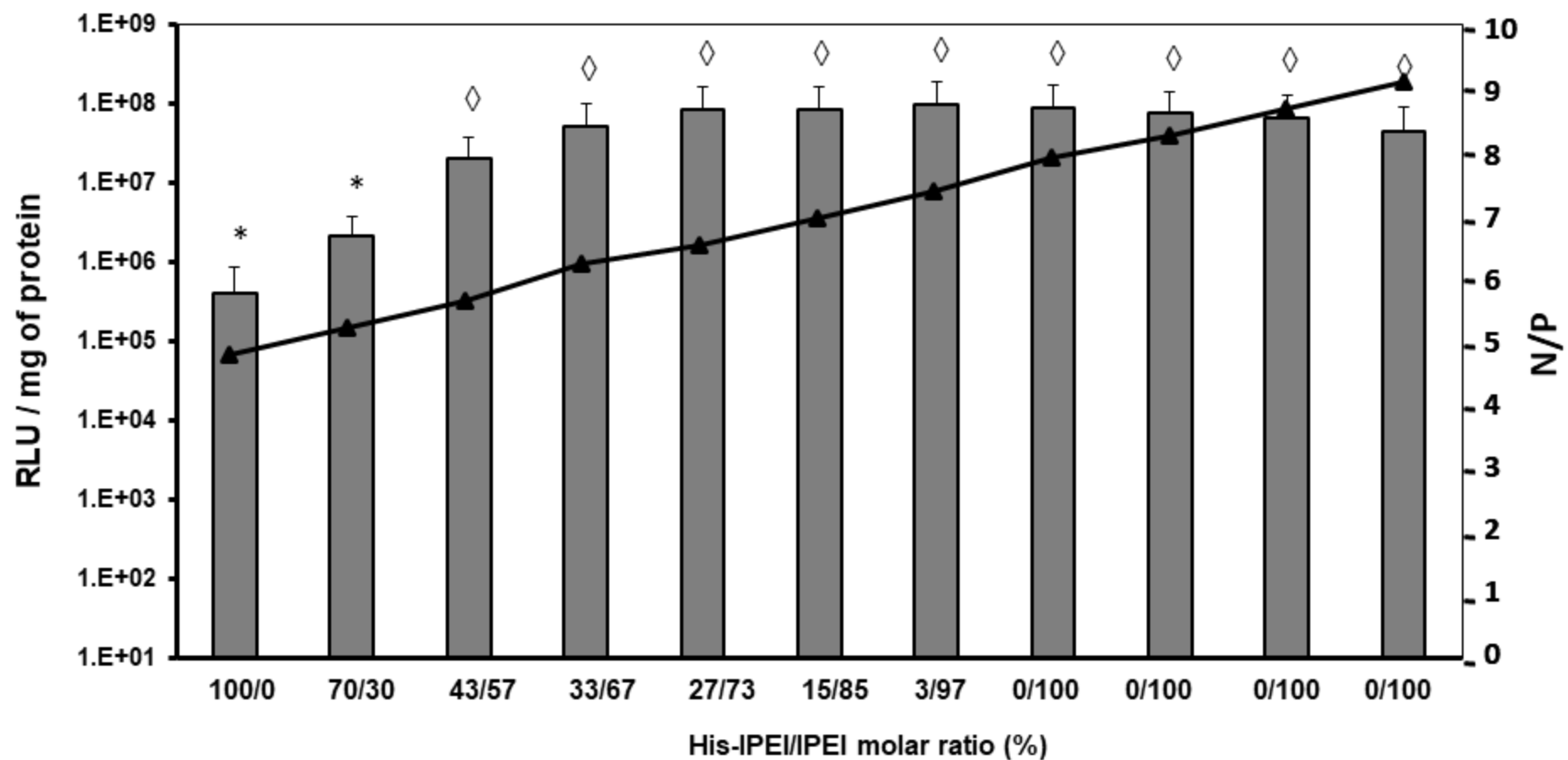


Fig 9

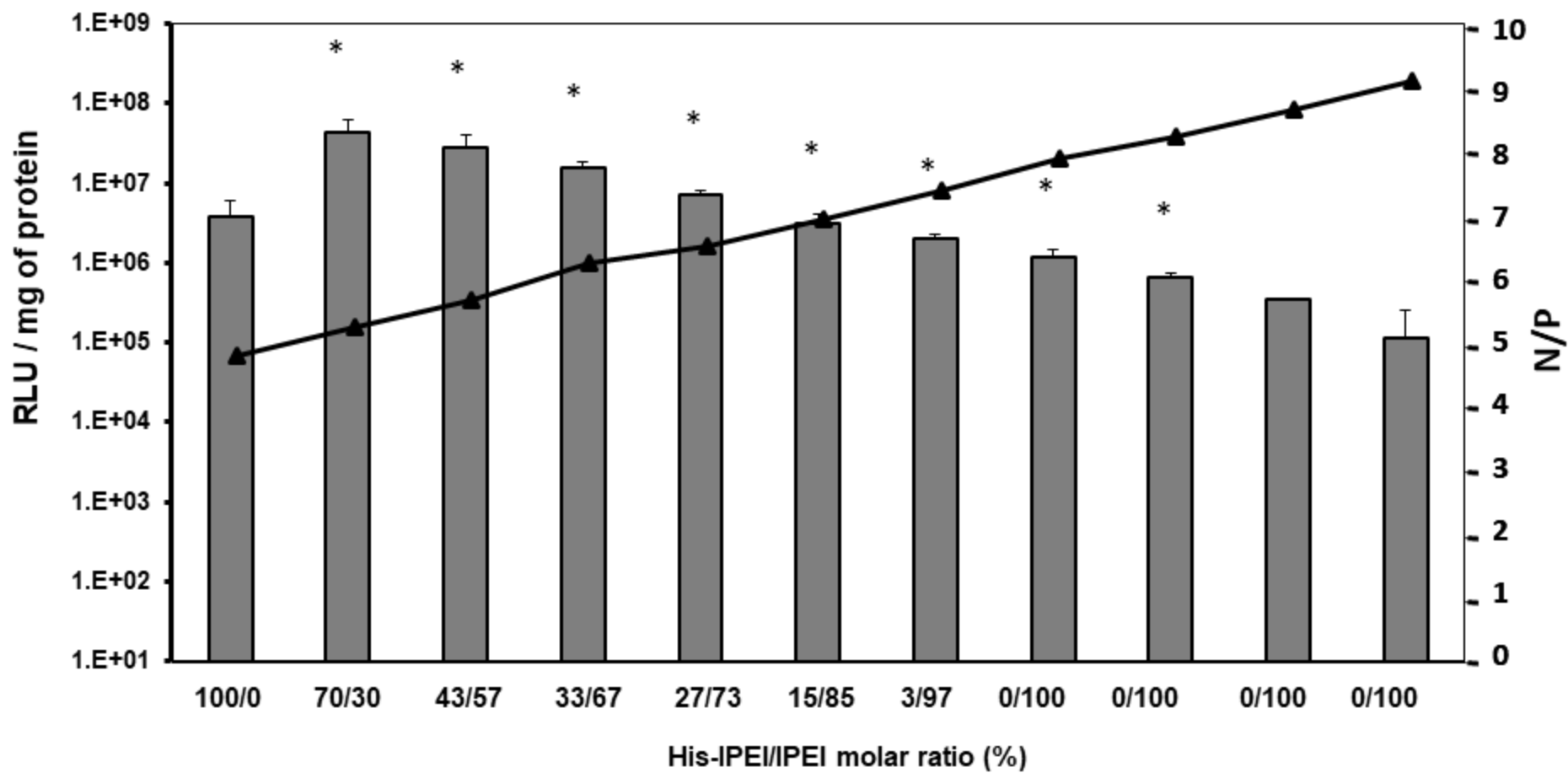


Fig 10

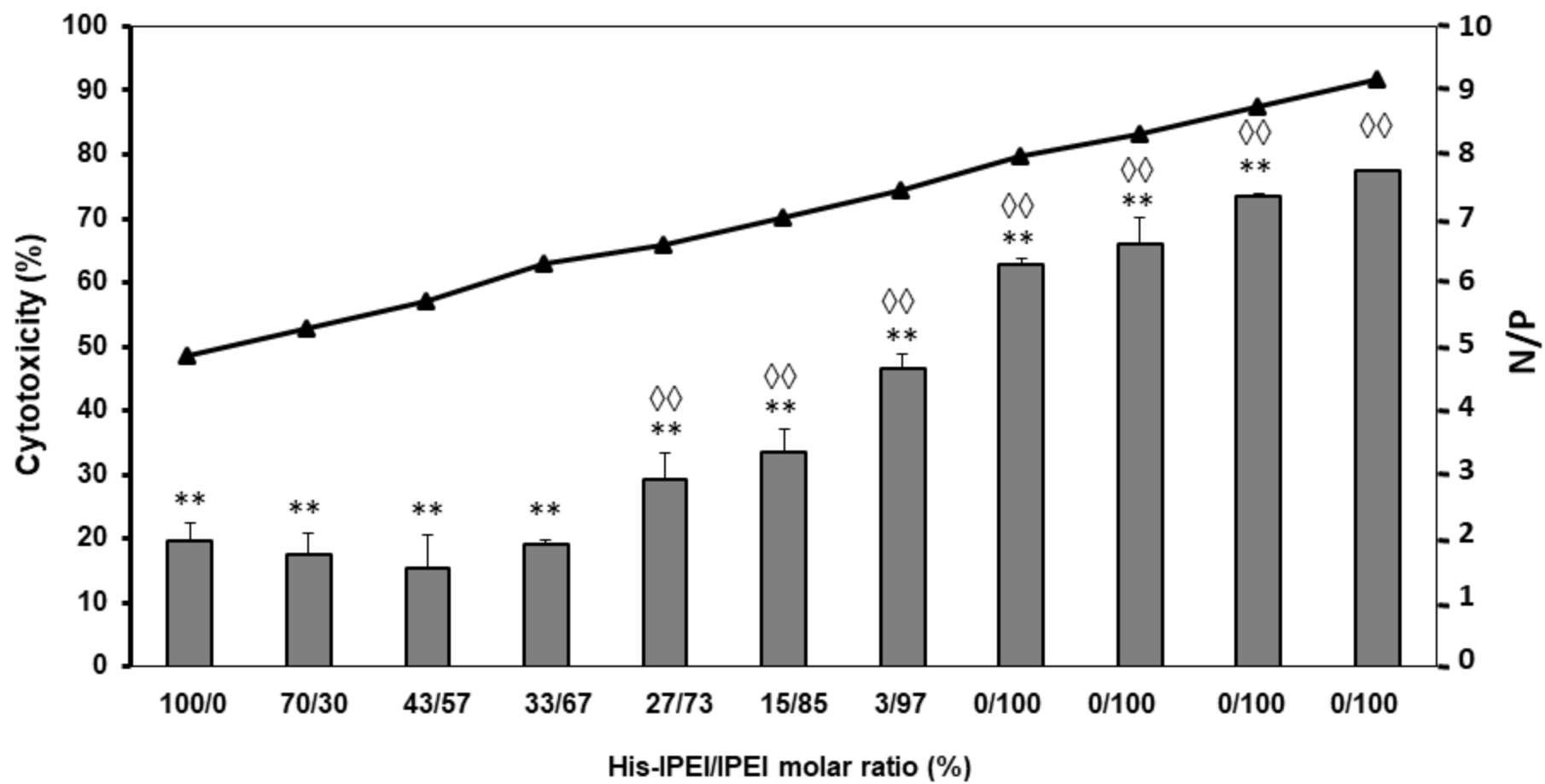
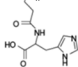
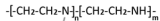


Fig 11

# (1)+(2) polyplexes



His-IPEI (1)



DNA

+



(1)

+

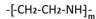


(2)

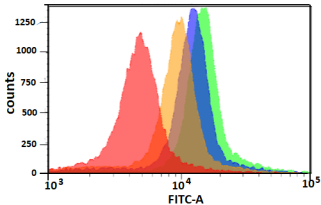
→



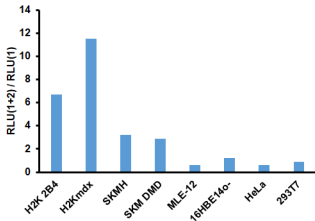
polyplex



IPEI (2)



Polyplex composition as function of the (1)/(2) ratio



Improved skeletal muscle cell transfection